Art. N° 388
Contribution COB N° 551

OCEANOLOGICA ACTA 1978 - VOL. 1 - N° 1

Hydrothermal deposits sampled by diving saucer in Transform Fault "A" near 37°N on the Mid-Atlantic Ridge, Famous area

Hydrothermal
Mineralogy
Geochemistry
Transform Fault
Submersible

Hydrothermal
Minéralogie
Géochimie
Faille Transformante
Submersible

M. Hoffert [a], A. Perseil [b], R. Hékinian [c], P. Choukroune [d],
H. D. Needham [c], J. Francheteau [c], X. Le Pichon [e]
[a] Centre de Sédimentologie et Géochimie de la Surface, Institut de Géologie,
1, rue Blessig, 67084 Strasbourg.
[b] Laboratoire de Minéralogie du Muséum d'Histoire Naturelle,
61, rue Buffon, 75005 Paris.
[c] Centre océanologique de Bretagne,
BP 337, 29273 Brest.
[d] Laboratoire de Géologie, Université de Rennes,
BP 25 A, 35000 Rennes.
[e] Centre National pour l'Exploitation des Océans,
BP 107 16, 75783 Paris Cedex 16.

Received 29/8/77, in revised form 5/10/77, accepted 10/10/77.

This paper is dedicated to B. C. Heezen (1924-1977) *who pioneered the use of submersibles for the study of the ocean floor.*

ABSTRACT

Deep-sea hydrothermal deposits were observed, mapped and sampled *in situ* with the submersible "Cyana" in the Famous area of the Mid-Atlantic Ridge. Two neighbouring fields, each covering an area of about 600 m^2, are associated with low, E-W trending sediment-covered ridges that lie at a depth of about 2 700 m close to the axis of Transform Fault "A". In each field the deposits are thicker (up to about 1 m) close to the small, fissure-like vents through which they were evidently delivered. Despite their heterogeneous composition, their mineralogical and chemical variations have an orderly pattern. The principal constituents are a green clay-rich material and Fe-Mn oxides in the form of black concretions. The relative abundances of these products vary with distance from the source-vent. The green clay-rich material, abundant near the vent, consists of hydromica, smectite and an amorphous Fe-Si compound. Further away, the Fe-Mn concretions, made up of rancieite and todorokite, are the dominant components.

The hydrothermal deposits from Transform Fault "A" have a consistently low Ni (20-270 ppm), Cu (26-275 ppm), Co (< 91 ppm) and Zn (5-126 ppm) content which sets them apart from known deep-sea metalliferous sediments, manganese nodules and Fe-Mn coatings of ocean floor basalts. The Fe-Mn coatings of basaltic rocks from Transform Fault "A" have a lower Si/Al ratio ($\simeq 1.6$) and a narrower range in their Fe/Mn ratio (2-3) than the hydrothermal deposits (Al/Si = 4-153 and Fe/Mn = 0.3-35).

Oceanol. Acta, 1978, **1**, 1, 73-86.

Contribution n° 551 du Département Scientifique, Centre Océanologique de Bretagne (Cnexo).

Dépôts hydrothermaux échantillonnés par la soucoupe plongeante « Cyana » dans la faille transformante « A » près de 37°N dans la zone Famous sur la dorsale médio-atlantique

RÉSUMÉ

La soucoupe plongeante « Cyana » a permis d'observer, de cartographier et d'échantillonner *in situ* des dépôts hydrothermaux dans la zone Famous de la dorsale médio-atlantique. Deux sites voisins, chacun recouvrant une surface d'environ 600 m^2 forment des monticules très peu sédimentés et allongés dans une direction E-W à une profondeur d'environ 2 700 m au voisinage de l'axe de la Faille Transformante « A ». Dans chaque site les dépôts sont plus épais (ils atteignent 1 m) près des griffons en forme de fissures. Les dépôts sont formés soit d'argile, en général de couleur verte, soit de concrétions noires de fer et de manganèse. Malgré leurs caractères hétérogènes la minéralogie et la chimie des dépôts montrent une zonation. L'abondance relative des dépôts varie avec la distance aux griffons : les dépôts de couleur verte enrichis en argile (smectite, hydromica et matériel amorphe enrichi en Fe-Si), sont abondants près des sorties; les concrétions de Fe-Mn deviennent abondantes au fur et à mesure que l'on s'en éloigne. Parmi les principaux produits de Fe-Mn notons la todorokite et la rancieite. Les dépôts hydrothermaux de la Faille Transformante « A » ont de faibles teneurs en Ni (20-270 ppm), Cu (26-275 ppm), Co (<91 ppm) et Zn (5-126 ppm) ce qui les différencie des sédiments métallifères, des nodules polymétalliques et des encroûtements de Fe-Mn des basaltes océaniques. Les encroûtements de Fe-Mn des basaltes prélevés dans la faille Transformante « A » ont un rapport Si/Al ($\simeq 1.6$) plus faible et une variation des rapports Fe/Mn plus limitée (2-3) que les dépôts hydrothermaux (Al/Si = 4-153 et Fe/Mn = 0.3-35).

Oceanol. Acta, 1978, **1**, 1, 73-86.

INTRODUCTION

The origin, detailed structural setting and diversity of hydrothermal deposits associated with young oceanic crust are currently attracting considerable interest (Scott *et al.*, 1974; Hajash, 1975; Moore, Vogt, 1976; Cann *et al.*, 1977). It is likely that hydrothermal circulation in the oceanic crust is more important than hitherto realized in generating a selective concentration of chemical elements, in alteration effects and in the chemical balance of sea water. Field observations of hydrothermal deposits were limited to subaerial exposures until two

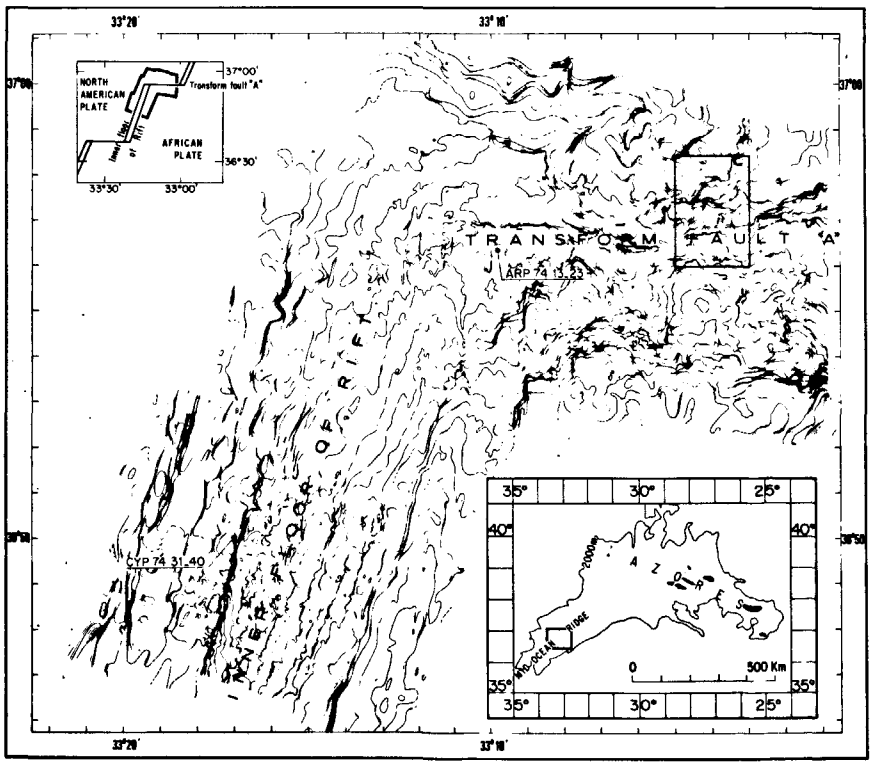

Figure 1

General bathymetric map of part of the Famous area after Renard et al. (1976). *The inset in the lower right shows the setting of the Mid-Ocean Ridge area with respect to the ridge and the Azores. The inset in the upper left shows the local setting of the mapped area. The two samples on the map are from the Rift Valley* (cyp 74-31-40) *and from the Western part of Transform Fault "A"* (ARP 74-13-23). *The open box in the bathymetric map is enlarged in Figure 2.*

hydrothermal fields were observed and sampled from the diving saucer "Cyana" in 1974 during the Famous (French American Mid-Ocean Undersea Study) operation in Transform Fault "A" near 37°N (Fig. 1, 2). Four dives were made on the two fields and two of these led to successful sampling. The two hydrothermal fields lie 200 m apart at a depth of 2 670-2 690 m (Fig. 2). They occur in a zone of active left-lateral strike-slip faulting, on the top of a scarp immediately to the south of the deepest portion of the Transform Valley where most of the transform motion is now occurring (Arcyana, 1975; Choukroune *et al.*, 1977).

The main purpose of this study is to describe the morphology, mineralogy and chemistry of the observed hydrothermal deposits. Chemical and mineralogical analyses of the deposits are used in conjunction with the structural setting of the samples to try to understand the origin of the various constituents forming the hydrothermal deposits. A comparative study of the Fe-Mn coatings of basaltic rocks found in the same general area was made in order to establish whether there is any direct relationship between the two types of deposit. Finally, a brief survey of the literature is made to see how the Famous hydrothermal deposits fit among similar deposits which have been described from other parts of the ocean.

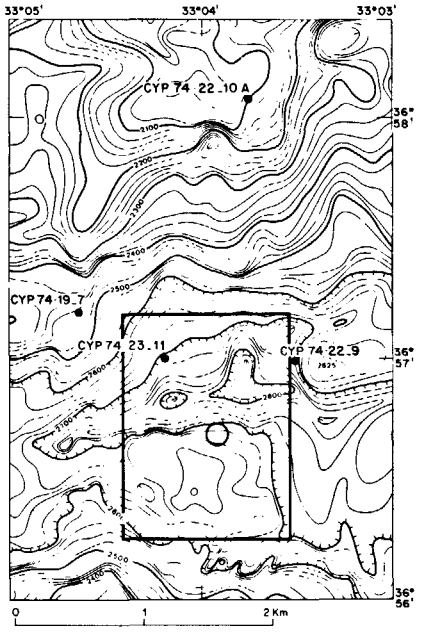

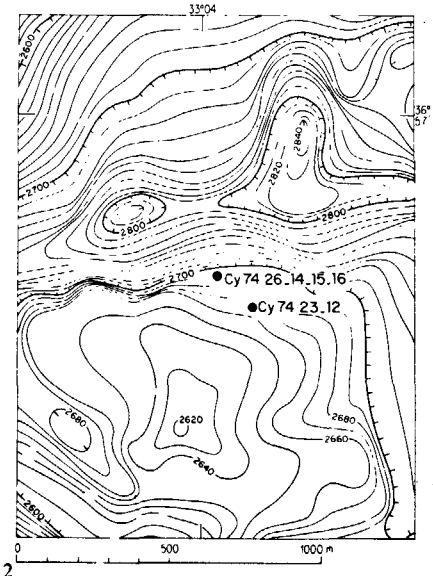

Figure 2

Left: Bathymetry in the median part of Transform Fault "A" with locations of basaltic samples selected for their Fe-Mn *coatings and location of hydrothermal area (open circle). Right: detailed bathymetry of the area outlined by box in left hand figure and locations of the two hydrothermal fields found during dives* Cy 74-23 *and* Cy 74-26.

FIELD OBSERVATIONS AND SAMPLING

The deposits from the two hydrothermal fields, each of which is associated with a vent, lie on sediment and form small E-W trending ridges. The ridges are asymmetrical with steeper-dipping northern ($\simeq 50°$) than southern slopes ($\simeq 20°$). The ridges are associated with faults. The vents are fissure-like (0.1-0.3 m wide) structures with an E-W orientation parallel to the elongation of the ridges (Fig. 3, 4 A) and, in both fields, lie towards the top of the north-facing slope. The vents can be followed for several meters but no obvious signs of activity were seen. Water sampling and temperature measurements made in the vicinity of the vents did not indicate any compositional or thermal anomalies. The hydrothermal deposits spread out in a fan-like fashion away from each vent. The samples collected during dives Cy 74-23 and Cy 74-26 consist of a variety of material, chiefly Mn and Fe oxides, smectite, semi-indurated sediment, and small fragments of basaltic rock, some of which are coated with the Fe-Mn oxides and clay (smectite) that appear to be of hydrothermal origin.

The thickness of the hydrothermal deposits decreases away from the fissure-like vents: from 100 cm to about 10 cm. Each field covers a surface area of about 600 m^2 (15×40 m) (Fig. 2). A schematic cross-section of one of the hydrothermal fields is shown in Figure 3. The tops as well as the southern slopes of the ridges are covered by

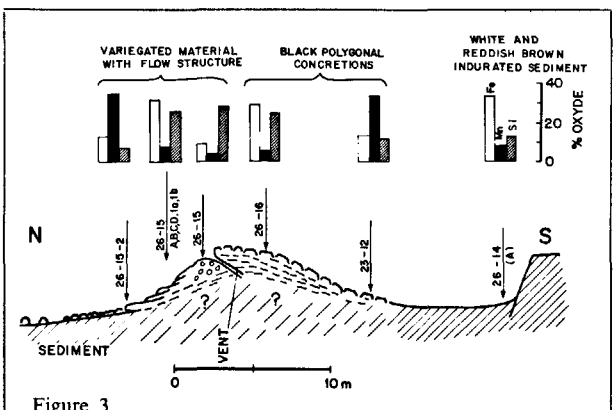

Figure 3

Schematic cross section of the western (Cy 74-26) *hydrothermal field showing the projected location of the sampling sites. All the sample numbers have the prefix* cyp 74 *corresponding to the "Cyana" dives of* 1974. *Sample* 23-12 (cyp 74-23-12) *was taken from the eastern hydrothermal field (Fig. 2) and was relocated in this profile according to its distance from the vent of site* cyp 74-23-12. *The circles near sampling site* 26-15 *indicate the presence of pisolith-like concretions.*

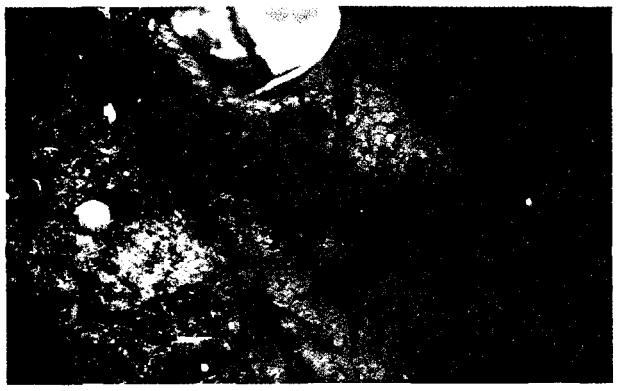

4 A

4 B

Figure 4

A) *Bottom photograph of the hydrothermal field found in Transform Fault "A" near 37°N on the Mid-Atlantic Ridge showing the fissure-like vent located on the northern slope of the field. The total length of the mechanical arm below the elbow is 52 cm (Fig. 5 A). The length of each petal-like segment of claw is 15 to 20 cm.*

B) *Top of the hydrothermal ridge showing a discontinuous type of deposit of polygonal appearance.*

dark, nearly black stratified deposits (samples 12 and 16) (Fig. 3, 4 B) which consist of unevenly distributed, scoria-like material with a polygonal outline. The appearance in the field is that of a desiccated mud-flat (Fig. 4 B). The polygonal-shaped concretions thin away from the vent, becoming lighter and assuming different shades of reddish-yellow and yellowish-green. Sample 12 taken about 10 m from the vent is made up of a black scoria-like Fe-Mn concretion together with yellowish-green material and associated with volcanic debris and with foraminifera showing epigenetic changes (Fig. 3, Table 1).

Near the vents and on the northern slopes of the hydrothermal ridges, the deposits form a continuous cover. They are more variegated than those from the southern slopes and have a travertine-like appearance with apparent flowage down the vent. There are black pisolitic-concretions (Fig. 3) with a geode-like zonation in cross-sections, appearing from the center outward as a change from black to rusty-red to yellowish-green and dark green (Table 1). Many of the concretions are associated with rock fragments (Table 1, sample 15).

The samples from the northern slope of the western hydrothermal deposit (15 A, 15 B, 15 C, 15 D, 15-1 and 15-2) were taken within a few meters of each other. The sample judged to be farthest from the vent is 15-2 and is located at a distance of about 7 m from it (Fig. 3). A sample of basaltic rock found at the center of a concentric concretion (15) was taken about 2 m away from the vent (Table 1, Fig. 3, 5 A). Looking at the interior of the fissure-like vents, the observer noted that the rusty red colored material is the most abundant here (Fig. 4 A).

The sediment on which the hydrothermal material of the western field was deposited consists dominantly of partially indurated white mud. A sample (14) taken about 20 m away from the vent on the southern slope of the ridge is made up essentially of coccoliths, debris of volcanic rock fragments, mineral grains, and clay particles (Table 1). One fragment of the semi-indurated material associated with the carbonate sediment (14) is made up of alternating laminae of Fe-Mn concretions having a metalliferous luster, and brownish-red isotropic material (cyp 74-26-14 A, Table 1). The deposits have not been disrupted by either erosion or faulting and their surfaces are almost entirely sediment free. This suggests a relatively young age. Radiochemical studies (Lalou *et al.*, 1977) on the Fe-Mn crust of the hydrothermal deposits from Transform Fault "A" indicate a maximum age of 45 000 years compared to a probable 1 million years for the underlying crust (Arcyana, 1975). It is interesting to note that no hydrothermal deposits were found in the main deep of Transform Fault "A". This could be because rapid infilling of the troughs by sediment and rock debris conceals hydrothermal deposits.

LABORATORY TECHNIQUES

Chemical analyses by arc spectrometry using an ARL quantometer were made at the University of Strasbourg following the method described by Besnus and Rouault (1973) and Besnus and Lucas (1970). This method consists of melting the sample in a mixture of lithium tetraborate and then introducing the melt into in a glycolated solvent. Trace elements were determined using graphite discs as described by Besnus and Lucas (1970). Na and K were determined by emission spectrometry (precision of $\pm 2\%$). Electron microscopy (Phillips EM 300) and infrared studies (Perkin-Elmer 577) were used for mineral identifications.

MINERALOGY OF THE HYDROTHERMAL DEPOSITS

The hydrothermal samples collected from Transform Fault "A" are heterogeneous and the intimate association of the various compounds within each sample made mechanical separation difficult. Interlayered structures and variously colored, irregularly bedded material occurs throughout the samples (Fig. 5 B). Most of the constituents forming the deposits are poorly crystalline. We divide the sampled hydrothermal deposits into two main categories according to the relative proportion of the black Fe-Mn concretions with respect to the clay-rich fraction:

1) clay-rich hydrothermal material made up essentially of various proportions of clays, hydromicas, opaques and amorphous material;

Table 1

Morphology and mineralogy of Transform Fault "A" hydrothermal deposits. Cy indicates the first two letters of the diving saucer "Cyana", p indicates that the sample was taken by a mechanical arm, 74 stands for 1974 and is followed by the dive and the samples numbers.

Sample No.	Setting	Structure and type of material	Mineralogy
cyp 74-23-12	Eastern site (Fig. 2). Sample taken from the flank of the small ridge	Polygonal black scoriaceous Fe-Mn concretions with very little clay	Todorokite, rancieite, manganite, Birnessite, kaolinite, illite, chrysotile, smectite
cyp 74-26-14	Western site (Fig. 2). Samples taken from the south flank of the ridge about 20 m away from the vent	Semi-indurated sediment with occasional Fe-Mn material	Coccoliths, calcite, clay, todorokite
cyp 74-26-14 A	Same location as cyp 74-26-14	Brownish-red crust (2 cm thick) covering the semi-indurated sediment (cyp 74-26-14)	Clay, todorokite, birnessite, cryptomelane, calcite
cyp 74-26-15-2	Western site. Sample taken on the northern flank of the ridge at about 7 m from the vent	Fe-Mn concretions with very little clay. Breccia.	Todorokite, rancieite, manganite, illite, chrysotile, smectite, calcite
cyp 74-26-15 A cyp 74-26-15 B	Western site. Samples taken on the northern flank of the ridge between 2 and 7 m from the vent	Yellowish-green clay-rich material. The clay shows lath-like and flaky structure	Hydromica, smectite, birnessite, todorokite, calcite
cyp 74-26-15 C	Same location as cyp 74-26-15 A	Black isotopic and clay-rich material surrounding a white-colored clay-rich material (cyp 74-26-15 *d*)	Smectite, hydromica, todorokite, pyrite
cyp 74-26-15 D	Same location as cyp 74-26-15 A	White-colored clay-rich material intermixed with sediment	Smectite, hydromica, todorokite, calcite, pyrite
cyp 74-26-15	Western site (Fig. 2). Sample of pisolith-like concretion taken on the northern flank of the ridge at about 2 m from the vent	Aphyric basaltic rock coated with yellowish-green clay-rich hydrothermal material found associated with pisolith-like concretions	Glass, olivine, serpentine
cyp 74-26-15-1 *a* cyp 74-26-15-1 *b*	Same location as cyp 74-26-15 A Same location as cyp 74-26-15 A	Dark-green clay-rich material intermixed with rusty-brown material	Hydromica, smectite, todorokite, manganite, pyrite
cyp 74-26-16	Western site (Fig. 1). Samples taken near the top of the ridge at about 3 m from the vent	Stratified yellowish-green clay-rich material with black Fe-Mn scoriaceous concretions	Smectite, hydromica, todorokite, rancieite, manganite, birnessite

2) black Fe-Mn concretions made up essentially of amorphous manganese bearing minerals.

These two major types of material appear to represent the end products of a compositional range. The gradual color changes observed probably correspond to transitional products between these two types.

The clay-rich hydrothermal material

The material represented by samples 15-1 *a*, 15-1 *b*, 15 A, 15 B, 15 C and 16 consist essentially of opaque flaky particles rich in Fe and Si and poor in Al (Fig. 5 A, 8) when compared to the other constituents. Micro-diffraction studies have shown that the opaques

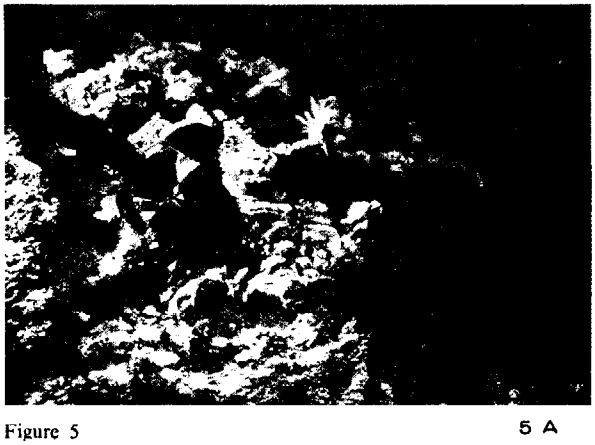

Figure 5 5 A

A) *North flank of hydrothermal ridge showing concentric concretions.*

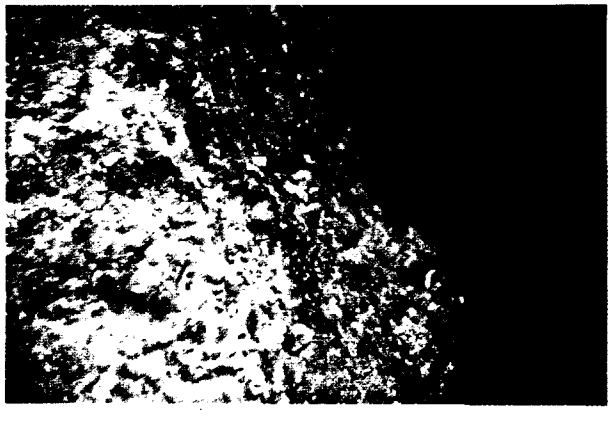

B) *Bottom color photograph of hydrothermal field located in Transform Fault "A" shows bedded deposits of* Fe-Mn *concretions (black) and clay-rich material (variegated).*

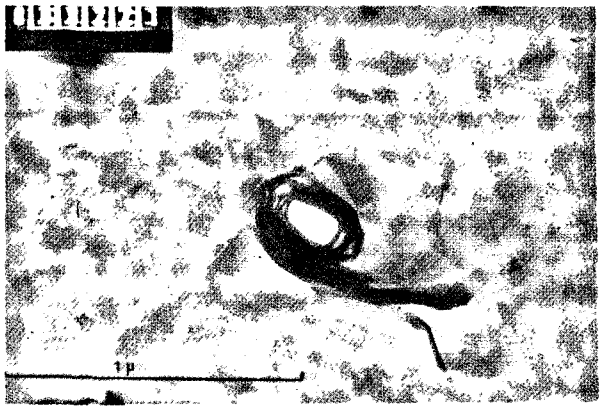

6 A

6 B

6 C

Figure 6

A) *Morphology of clay particles viewed with an electron microscope (transmitted light). Two types of particles are seen: a lath-like particle of about* 0.1 μm *and a flaky-type particle of about* 0.5 μm.

B) *Morphology of hydromica viewed with an electron microscope. The flaky type of structure is that of glauconite-celadonite.*

C) *Microphotograph of folded flakes of smectite in sample* cyp 74-26-15.

have a rolled, sheet-like structure with a lattice spacing of their *d* (001) atomic planes of 10.1-10.6 Å, and X-ray diffractograms show 10.2-10.6 Å peaks. These parameters correspond to the structural characteristics of hydromica (glauconite-celadonite) (Fig. 6 B, 8). The green, opaque and flaky particles are most abundant in samples 15-1 *a*, 15-1 *b* and 15 A, which consist of rusty brown and black material that is dark green when freshly fractured (Table 1). In addition, the yellowish-green clay-like material is made up of fine lath-like particles whose lattice is of the clay-mineral type and has the following atomic cell dimensions: $d\,(020) = 4.54\ \text{Å} \pm 0.03$; $d\,(200) = 2.65\ \text{Å} \pm 0.03$; $d\,(060) = 1.52$ Å. The lath-like particles are rich in Fe and Si and poor in Mg and K. X-ray diffraction study of the clay fraction indicates the presence of expandable clay (16 Å peaks). Results of heat treatment do not reveal the presence of interstratified chlorite layers. A similar type of sample from Transform Fault "A", studied by Thompson *et al.* (1975), showed the presence of Fe-rich clay. Such features are typical of smectite of nontronite composition (Fig. 6 C). These lath-like particles are found in all the hydrothermal samples. Depending upon the relative amount of hydromica or smectite, the clay-rich hydrothermal material assumes different shades of green. A dark green clay-rich hydrothermal material made up mainly of hydromica is represented by samples 15-1 *a*, 15-1 *b* and 15 A, while other yellowish-green hydrothermal material is rich in smectite (Table 1). The small amounts of manganese minerals found in association with the clay-rich hydrothermal deposit consist mainly of todorokite and birnessite (Table 1).

The black Fe-Mn concretions

These occur either as gel-like inclusions and/or interlayered laminae of todorokite [(Mn, Ca) $Mn_2O_9 . 2\ H_2O$] and rancieite (RO, 4 MnO_2, 4 H_2O). Rancieite is distinguished from todorokite by its strong pleochroism. Infrared observations of the gel-like inclusions forming the nucleus of the Fe-Mn concretions show that they are isotropic and have a 3 μm-thick band of water. The gel-like material probably crystallizes into todorokite and rancieite with which it is always associated. The proportion of gel and of the crystallized todorokite-rancieite pair is constant throughout the various samples. In addition, small amounts of kaolinite, illite and chrysotile are found within the black Fe-Mn concretions (Table 1). Criss-cross lamellae of manganite (*x*-MnOOH) were found to occur in the concretions (surface coating of sample 15 (Fig. 7 A, B). Birnessite also was found to fill small cavities of the Fe-Mn concretions (sample 12, Table 1).

Miscellaneous material

Semi-indurated sediment (14) consisting of coccoliths, calcite and clay and coated with alternating laminae of todorokite and brownish-red clay-rich material (14 A) (Table 1) were sampled during dive Cyp 74-26. Sample 14 A contains an Fe-Mn gel-like amorphous material which occurs at the center of a concretion. Birnessite was found to form the major constituent of this concretion. Fine laths of smectite, reddish-brown fibers of manganite and occasional cryptomelane (MnO_2) also occur in sample 14 A (Table 1).

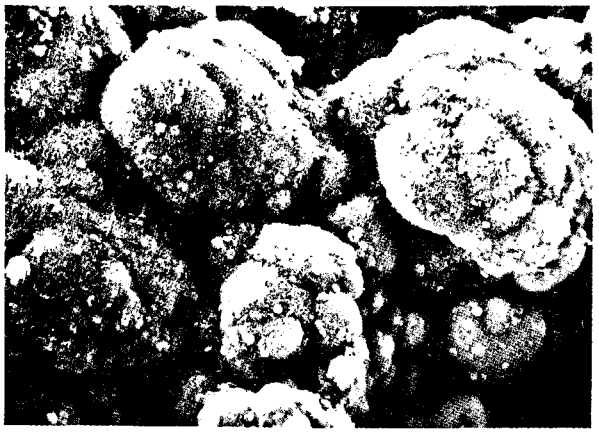

7 A

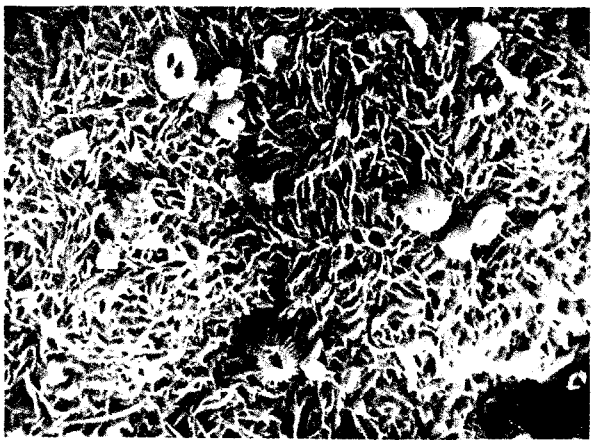

7 B

Figure 7

A) *Microphotograph of manganite* (sample cyp 74-26-15) (*electron microscope: photo magnification* × 500).

B) *Microphotograph of the same sample of manganite* (cyp 74-26-15) *viewed under higher magnification* (*photo magnification* × 2 800).

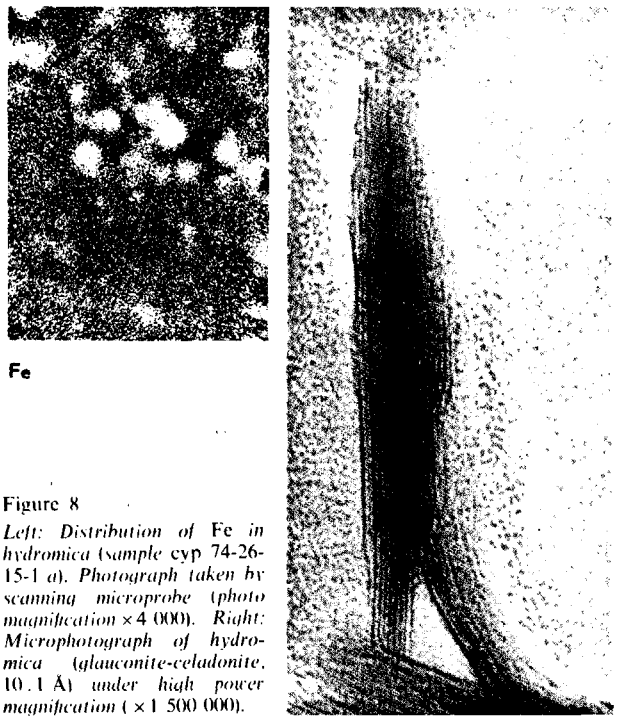

Fe

Figure 8

Left: Distribution of Fe *in hydromica* (*sample* cyp 74-26-15-1 *a*). *Photograph taken by scanning microprobe* (*photo magnification* × 4 000). *Right: Microphotograph of hydromica* (*glauconite-celadonite*, 10.1 Å) *under high power magnification* (× 1 500 000).

Some basaltic rock fragments were found to be coated with yellowish-green, dark-green and brownish red clay-rich hydrothermal material. One of these (15) was studied, and consists of a relatively fresh glass with incipient crystallization shown by a grid-like texture. A few olivine crystals, some of them replaced by serpentine, were recognized.

CHEMISTRY OF THE HYDROTHERMAL DEPOSITS

Most of chemical analyses were carried out on the bulk material. In a few cases the analyses refer to mechanically separated portions of individual samples (Table 2). In general the heterogeneous aspect of the different deposits makes it difficult to compare their chemistry. However, the differences are large enough to permit some distinctions to be drawn between groups that were recognized on the basis of mineralogical criteria.

The clay-rich hydrothermal deposits

These are grouped together regardless of their color. They are all rich in Fe_2O_3 (32-40 %) and SiO_2 (36-46 %) and, in most cases, poor in transitional metals (Table 2). Iron most commonly occurs in the lattice of the clay minerals. Most of the Mn content (7 705-82 811 ppm) of the clay-rich hydrothermal material is mainly due to the presence of manganiferous compounds (todorokite-manganite-birnessite) (Tables 1, 2). The yellowish-green, clay-rich hydrothermal material (15 A, 15 B, 16, 15-1 *a*) is the most depleted in Ni (2-33 ppm), Co (2-9 ppm), Zn (5-9 ppm), and Cu (46-88 ppm) with respect to the other types of deposits (Table 2). Among the clay-rich hydrothermal material (15 A, 15 B, 16, 15-1 *a*) is the most depleted in Ni (2-33 ppm), Co (2-9 ppm), Zn (5-9 ppm), and Cu (46-88 ppm) with respect to the other types of deposits (Table 2). Among the clay-rich hydrothermal material, there are samples (15-1 *b*, 15 C and 15 D) which have a higher Ni (66-116) and Zn (24-79 ppm) content than those mentioned above (Table 2). Since pyritic material was observed to occur in these samples, it is likely that the relatively high Zn and Ni content could be due to the presence of sulphides. Most of the clay-rich hydrothermal material is depleted in Al_2O_3 (< 1 %) except in samples 15 C and 15 D which have an alumina content of 3-6 percent (Table 2). The relatively high Al_2O_3 content of these two samples could be attributed to the presence of silicate minerals such as plagioclase, and the alumina increase of these samples is indeed accompanied by a relatively high CaO (4-6 %) content (Table 2). The brownish-red, clay-rich hydrothermal material (14 A), made up of smectite, Fe-Mn minerals and cryptomelane, has a higher Mn (82 811 ppm) and transitional metal contents (V = 472 ppm, Ni = 225 ppm, Zn = 84 ppm, and Cu = 135 ppm) than the other clay-rich hydrothermal material (Tables 1, 2). The greater abundance of these transitional metals is explained by the higher proportion of manganiferous compounds which, in turn, makes this type of material the closest among the clay-rich deposits to the Fe-Mn concretions (Table 2).

Table 2

Chemical analyses of hydrothermal deposits and associated material from Transform fault "A". (IGN) indicates ignition loss at 1 000°C.

	Fe-Mn-rich concretions			Clay-rich hydrothermal material							Miscellaneous	
Weight (%)	cyp 74-23-12 black	cyp 74-26-15-2 black	cyp 74-26-15-1 *a* dark green	cyp 74-26-15-1 *b* dark green	cyp 74-26-15 A yellowish green	cyp 74-26-15 B yellowish green	cyp 74-26-16 yellowish green	cyp 74-26-15 C black	cyp 74-26-15 D white	cyp 74-26-14 A brownish red	cyp 74-26-14 sediment	cyp 74-26-15 basalt
SiO_2	16.6	8.7	45.5	36.4	30.2	41.9	44.4	41.0	39.0	24.7	1.7	49.6
Al_2O_3	1.7	0.7	0.2	0.4	0.2	0.2	0.2	3.2	5.9	0.4	0.5	15.7
Fe_2O_3	16.3	13.7	37.9	38.6	32.3	35.1	35.6	29.9	20.8	40.6	1.1	8.8
Mn_3O_4	37.2	40.3	1.07	3.78	6.68	4.69	3.88	4.69	4.01	11.5	0.18	0.18
MgO	3.7	2.68	2.91	2.73	2.77	2.72	2.84	4.39	5.24	2.92	0.68	8.42
CaO	2.3	7.3	0.6	2.9	2.9	1.2	0.8	4.4	9.5	3.0	51.7	10.8
Na_2O	2.47	1.47	1.71	1.70	1.93	1.91	1.84	2.13	1.83	1.75	0.09	2.05
K_2O	0.97	0.28	3.23	2.77	3.00	2.80	3.35	2.28	1.55	1.76	0.05	0.59
TiO_2	0.08	0.04	0.02	0.02	0.02	0.02	0.02	0.20	0.38	0.03	0.05	0.85
IGN	15.93	20.11	6.22	9.53	9.13	7.94	6.95	8.14	9.94	12.89	42.9	0.94
TOTAL	97.25	95.28	99.14	98.81	98.81	98.46	99.66	100.33	98.15	99.55	98.86	97.93
Fe Mn	0.43	0.33	34.45	9.93	4.70	7.27	8.93	6.19	5.04	3.43	5.92	47.38
Si Al	6.55	8.35	152.79	61.11	134.93	140.64	149.07	8.60	4.44	41.46	2.29	2.12
Sr (ppm)	353	615	59	300	223	221	149	257	217	383	383	102
Ba	589	703	43	63	73	100	56	101	72	122	6	313
V	321	108	5	270	27	30	48	101	117	472	5	–
Ni	570	172	2	116	20	28	33	66	71	225	2	–
Co	91	73	2	8	9	2	2	10	27	10	2	–
Cr	13	9	4	8	10	11	9	62	84	4	2	–
B	204	170	75	529	532	576	592	461	293	442	5	–
Zn	126	40	6	36	5	6	9	24	79	84	5	8
Ga	5	9	2	5	5	5	5	5	13	5	2	–
Cu	275	137	46	88	64	66	49	73	60	135	26	100
Mn	267 877	290 200	7 705	27 219	48 096	33 768	27 939	33 768	28 876	82 811	1 296	1 296

The black Fe-Mn concretions

These concretions, rich in manganese (Mn = 26.8-29 %; samples 12 and 15-2) (Table 2) were referred to, in the mineralogy section, as the Fe-Mn concretions and are characterized by higher values of Ni (122-570 ppm), Cu (137-275 ppm) and Ba (589-703 ppm) than the other hydrothermal deposits (Table 2). The iron component of the concretions probably occurs as amorphous hydrated Fe oxide and/or as constituent of the gel-like material.

Miscellaneous material

This includes a semi-indurated carbonate-rich sediment (CaO = 51.7 %) with an ignition loss (mainly H_2O+CO_2) of 42.91 % and completely free of hydrothermal material, except for the surface coating of the brownish-red clay-rich material (14 A) described above (Table 1). In addition, a basaltic rock fragment (15) was found intermixed with the yellowish-green hydrothermal deposits. It showed a high ignition loss at 110°C (4.47 %) which is due to the occurrence of serpentine as an alteration product of olivine. The analysed trace element content of this basalt: Cu (100 ppm), Ba (313 ppm) and Sr (102 ppm) differs from that found in the yellowish-green hydrothermal material itself.

MODEL OF ZONATION

The major individual components forming the hydrothermal deposits can be physically separated into clay, hydromica, amorphous material and the various Fe-Mn oxides and hydroxide compounds (todorokite, manganite, rancieite, birnessite, cryptomelane). This observed mineralogical diversity reflects partly the chemical separation which occurs between the different phases of Fe, Mn and Si. In the field, this is expressed by the relative abundance of the variegated, clay-rich Fe-Si material near the vents and of the black Fe-Mn concretions further away from the vents (Fig. 3). It is worthwhile to note that, among the various types of deposits encountered, the association of amorphous gel-like material and of manganese minerals changes with distance away from the vents as follows: gel-manganite, gel-todorokite, gel-rancieite, birnessite-rancieite, and gel-cryptomelane (Table 1, Fig. 3).

Chemical zonation of hydrothermal fields in the ocean has been mentioned by Bonatti *et al.* (1972 *a*, *b*, *c*) and can be explained by a model proposed by Krauskopf (1957) in which Fe precipitates more rapidly than Mn during hydrothermalism. Experimental work (Hajash, 1975; Bischoff, 1972) has demonstrated that the formation of smectite from basaltic rocks in contact with sea water at a fairly high temperature ($\simeq$ 200°C) leads to the depletion of Mg^{2+} in the water. This would lower the pH, and the presence of Fe in the solid phase would promote a reducing environment (Michard, 1975). In this scheme a relatively hot acid solution with Fe^{2+} becomes alkaline on contact with the sea water, which is depleted in Mg^{2+}, and the Fe^{2+} precipitates. Because there is a deficiency in oxygen, the $Mn_4{}^{2+}$ will stay in solution and, when the solution cools down, Si will precipitate. This could explain the Fe-Si enrichment near the vent and the Mn increase away from it.

Table 3

Chemical analyses of Fe-Mn *coatings separated from the margins of basaltic rocks from Transform Fault "A" and from the Rift Valley near* 36°50'N (cyp 74-31-40). *ARP indicates a sample taken by the bathyscaphe "Archimède" in the Western part of Transform Fault "A"* (ARP 74-13-23; *Arcyana*, 1975). *Total iron was calculated as* Fe_2O_3 *and the total manganese as* Mn_3O_4. IGN *is ignition loss at* 1 000°C.

	ARP 74-13-23	cyp 74-19-7	cyp 74-22-9	cyp 74-22-10 *a*	cyp 74-23-11	cyp 74-31-40
SiO_2	8.6	7.9	7.4	7.4	8.8	13.0
Al_2O_3	4.6	4.6	3.5	4.5	5.2	7.7
Fe_2O_3 total	30.3	34.5	28.8	36.7	38.1	33.2
Mn_3O_4	10.4	14.1	12.8	17.2	13.4	11.0
MgO	2.31	2.97	3.11	3.66	2.99	3.53
CaO	7.5	11.2	7.3	7.3	8.3	9.1
Na_2O	0.88	0.80	0.90	1.28	1.34	1.29
K_2O	0.21	0.11	0.15	0.20	0.22	0.23
TiO_2	1.10	1.34	1.27	1.78	1.43	1.64
IGN	31.64	21.54	33/61	18.21	18.53	16.86
TOTAL	97.54	99.03	98.61	48.23	98.31	97.55
Fe/Mn	2.82	2.37	2.18	2.07	2.76	2.93
Si/Al	1.65	1.51	1.86	1.45	1.49	1.49
Srppm	2 530	2 826	2 258	3 190	2 535	1 745
Ba	752	973	744	916	850	665
V	1 370	1 570	1 300	1 500	1 500	1 300
Ni	650	780	650	1 100	950	700
Co	1 800	2 500	2 300	3 000	2 300	1 900
Cr	71	110	86	75	82	190
B	328	393	276	400	400	345
Zn	318	424	279	380	380	300
Ga	27	27	20	20	16	< 5
Cu	410	353	300	393	490	500
Mn	74 890	101 534	92 172	123 857	96 493	79 211

COMPARISON OF THE HYDROTHERMAL DEPOSITS WITH Fe-Mn COATINGS ON BASALTIC ROCKS

In order to evaluate the possible influence of hydrothermal activity on Fe-Mn coatings found on the surfaces of basaltic rocks in the median part of Transform Fault "A", a few samples collected in different structural settings less than 2 km away from the hydrothermal fields (cyp 74-19-07; cyp 74-22-09; cyp 74-23-11; cyp 74-22 10 A) were analyzed (Fig. 2). We also analyzed samples collected further west in the Transform Valley (sample ARP 74-13-23) and from the top of the deepest escarpment of the inner west wall of the Rift Valley near 36°50'N (sample cyp 74-31-40; Arcyana, 1975, 1977) (Fig. 1). There is a clear difference between the bulk composition of the Fe-Mn coatings of the basaltic rocks and that of the Fe-Mn material of the hydrothermal deposits (Table 3). In particular the Fe/Mn and Si/Al ratios are 2-3 and 1.5-1.9 respectively for the Fe-Mn coatings, and 0.3-35 and 6-150 for the hydrothermal deposits (Table 3). Further, the transitional metals of the Fe-Mn coatings of the rocks have higher values of TiO_2 (>1 wt%), Ni (>600 ppm), Cu (>300 ppm), Zn (>300 ppm) and Co (>1 800 ppm) than those found for the hydrothermal deposits (Table 3). On the other hand, the boron content of the Fe-Mn coatings of the basaltic rocks is intermediate (276-400 ppm) between that of the Fe-Mn concretions (170-204 ppm) and that of the most clay-rich hydrothermal material (293-592 ppm) (Tables 2, 3). At low temperatures clay minerals absorb boron from sea water, (Levinson, Ludwick, 1966). It has been shown that, with weathering, ocean floor basalt also adsorb boron from sea water (Thompson, Melson, 1970). Gallium (Ga) shows a positive correlation with alumina. A larger Al_2O_3 content in most of the Fe-Mn coatings of the basaltic rocks (4-6%) compared to that of the hydrothermal deposits (Al_2O_3 = 0.2-1.7%) is accompanied by a larger Ga content (16-27 ppm and 2-13 ppm respectively) (Tables 2, 3). This correlation suggest that Ga may enter into the lattice of the alumina-silicate material associated with the Fe-Mn and palagonite coatings of the basaltic rocks.

The difference in composition between the Fe-Mn concretions of the hydrothermal deposits and the Fe-Mn coatings on the nearby basaltic rocks highlights the whole question of what specific processes are responsible for the formation of Fe and Mn-rich deposits in the deep-sea, and for their associated minor element concentrations. At first view, one simply attributes the observed differences to the operation of two distinct processes (hydrothermalism and cold-water authigenesis). However, there seems to be no evidence for excluding the possibility that there is some association between the formation and composition of the coatings we have studied and the local addition by hydrothermalism of various elements into circulating bottom waters. Similarly, one might speculate that there could be some connection between palagonitization (e. g. Moore, 1966; Hékinian and Hoffert, 1975) and the availability of particular elements (e. g. Al and Ti) which entered into the Fe-Mn coatings we have analysed.

COMPARISON OF THE CHEMISTRY OF TRANSFORM FAULT "A" SAMPLES AND OTHER OCEANIC METALLIFEROUS DEPOSITS

Reviews of the compositional diversity and geographic distribution of oceanic metalliferous deposits have been made by Cronan (1975 *a*) and Rona (1977). For the purpose of comparative study we have put emphasis only on the metalliferous deposits from the ocean floor which have been studied in some detail. Because chemical comparison between various metalliferous deposits is a difficult task (since most material recovered from the ocean floors is heterogeneous), we will simply group the deposits in a general way according to their depositional environment and their inferred origin:

1) hydrothermal deposits *sensu stricto* which result from hot fluids circulating in the oceanic crust and debouching on the ocean floor and which are associated with volcanic terrain. Examples of this type of deposit occur in Transform Fault "A" (Arcyana, 1975 and this paper), on the Mid-Atlantic Ridge near 26-30°N (TAG area; Scott *et al.*, 1972, 1974), on the East Pacific Rise near 10°S (Bonatti, Joensuu, 1966), on the Galapagos spreading center (Moore, Vogt, 1976), and in the Median Valley in the Gulf of Aden (Cann *et al.*, 1977). So far, these deposits have been found only along divergent plate boundaries and associated transform faults;

2) metalliferous sediments which are formed by interaction of hot hydrothermal emanations with sediments, by biological activity, by diagenesis, by hydrogenous processes or by a combination of any of the above. Examples of this type of deposit are found in the Red Sea brine area (Bischoff, 1969), and areas in the south east Pacific (including Bauer Deep; Heath, Dymond, 1977). The deposits thus occur both in zones of divergent plate boundaries and in mid-plate areas;

3) hydrogenous deposits which result from the precipitation of metallic elements from sea water after transport in an oxidized environment and from the remobilization of elements during diagenesis (Cronan, 1975 *b*). This type of deposit includes the polymetallic nodules and the Fe-Mn coatings.

We will consider mainly bulk sample data and refer to selected parameters (Fe/Mn and Si/Al; Ba, Sr, Zn, Cu, Ni and Co contents) in order to compare deposits associated with various tectonic environments.

Fe/Mn and Si/Al

The Fe/Mn and Si/Al ratios (Fig. 9) serve to distinguish the hydrothermal deposits of Transform Fault "A" from deep-sea polymetallic nodules and from Fe-Mn coatings of basaltic rocks. The polymetallic nodules from the Pacific Ocean floor have values of Fe/Mn (>4) and of Si/Al (>5) similar to those of the Fe-Mn coatings of pillow lavas collected in the Famous area (Fig. 9). The clay-rich hydrothermal material from Transform Fault "A" (26-15 A, 26-15 B, etc. in Fig. 9) is closest, as far as Fe/Mn and Si/Al are concerned, to the yellowish-green friable material (mixture of smectite and Fe-Mn oxide; E in Fig. 9) from the Rift Valley in the Gulf of Aden (class "*d*" material of Cann *et al.*, 1977). In addition the ferromanganese oxides from the Gulf of Aden (C in Fig. 9; class "*c*" of Cann *et al.*, 1977) show values of Fe/Mn and Si/Al similar to those for the Fe-Mn concretions of Transform Fault "A" (23-12 and 26-15-2 in Fig. 9). The ratios for the mixture of smectite with ferromanganese oxides (class "*e*" of Cann *et al.*, 1977) are similar to those of the yellowish-green clay-like material from Transform Fault "A" (Fig. 9).

Barium and strontium

These elements are sensitive to weathering and enter readily into aqueous bicarbonate solutions. The Sr and Ba content of the Fe-Mn coatings of pillow-lavas is higher (1 500-4 000 ppm and 600-1 000 ppm respectively) than that of the hydrothermal deposits from Transform Fault "A" (59-615 ppm and 72-703 ppm respectively; Table 2). A sediment (26-14) from Transform Fault "A" shows a Sr content (1 383 ppm; Table 2) as high as that of the Fe-Mn coatings on the basaltic rocks. In addition the Fe-Mn concretions show Sr values (353-615 ppm) which are similar to those of the clay-rich hydrothermal deposits of Transform Fault "A" (Table 2). High Sr values were also reported for the metalliferous sediment of the Bauer Deep (up to 1 500 ppm; Fig. 10; Sayles, Bischoff, 1973). These latter deposits are also very rich in Ba (3 700-2 300 ppm; Sayles, Bischoff, 1973; Dymond *et al.*, 1973). It was further reported that these deposits from the Bauer Deep contain abundant manganese nodules. The high Sr content in metalliferous deposits might be due to Sr infiltration from sea water and/or from sediment into a porous environment and/or from the weathering of basaltic glass. The precipitation of barium might take place in an oxidized environment rich in manganese dioxide. In the Fe-Mn concretions of Transform Fault "A" the samples most enriched in Ba are those containing the highest amount of Mn (sample 12 and 15-2; Table 2; Fig. 10). The difference in barium content between the clay-rich hydrothermal material and the Fe-Mn concretions of Transform Fault "A" suggests that barium has a hydrothermal origin (Table 2). This was emphasized for the Fe-Mn-Ba rich deposits of the Afar region (Bonatti *et al.*, 1972 *b*).

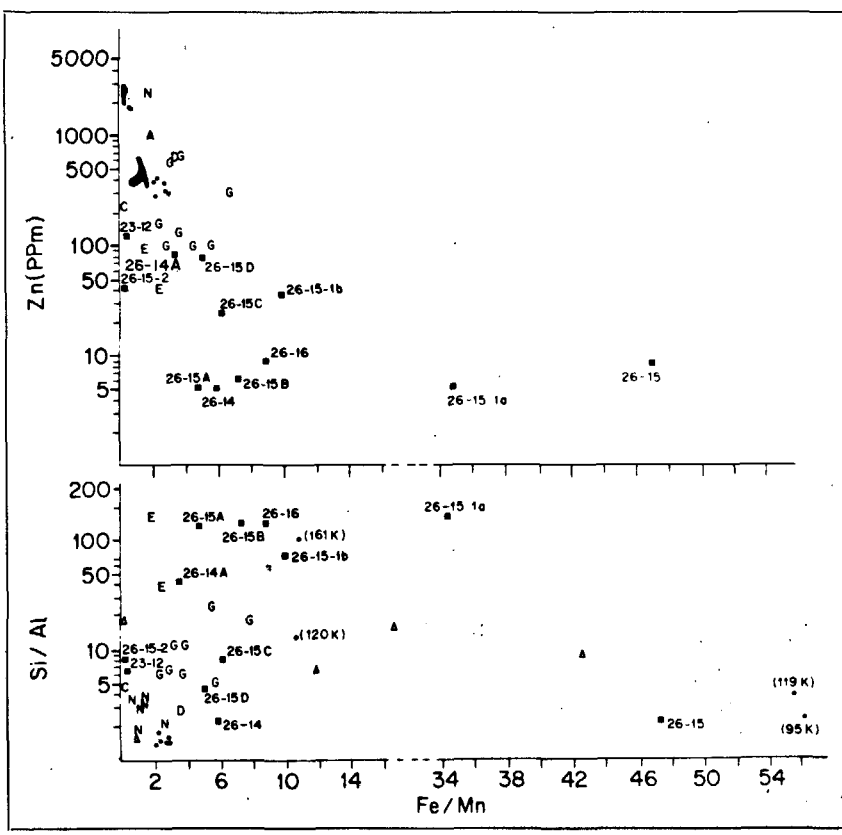

Figure 9

Si/Al *and* Zn-Fe/Mn *variation diagram showing field of hydrothermal deposits from Transform Fault "A"* (■). *The* Fe-Mn *coatings of basaltic rocks from the Rift Valley, from the Rift Valley-Transform Fault intersection zone and from Transform Fault "A" are also shown* (●). 161, 120, 119 *and* 95 K *are average compositions of metalliferous sediments from the Red Sea (Bischoff,* 1969). A) *indicates a manganese crust from the Atlantis F. Z. (Scott* et al., 1974). G) *indicates samples of the ferromanganoan deposit from the Bauer Deep (Sayles, Bischoff,* 1973). D) *is the average of the* Fe-Mn *rich deposit from DSDP site* 37, 38, 39, *(Dymond* et al., 1973) *collected in the central North Pacific Ocean.* (▲) *indicates manganese crust from a Pacific Ocean seamount dredge* (Amph D2: *Bonatti, Joensuu,* 1966) *located in the Bauer Deep.* N) *are samples of manganese nodules from the Pacific Ocean (Fein, Morgenstein,* 1973; *Tanticelli, Perkins,* 1973). F) *indicates the* Mn-*rich deposits from the Afar region (Bonatti* et al., 1972 *a*). C) *corresponds to ferromanganese oxide from the Gulf of Aden and* E) *to a mixture of* Fe-Mn *oxide and* Fe *oxide from the Gulf of Aden (Cann* et al., 1977).

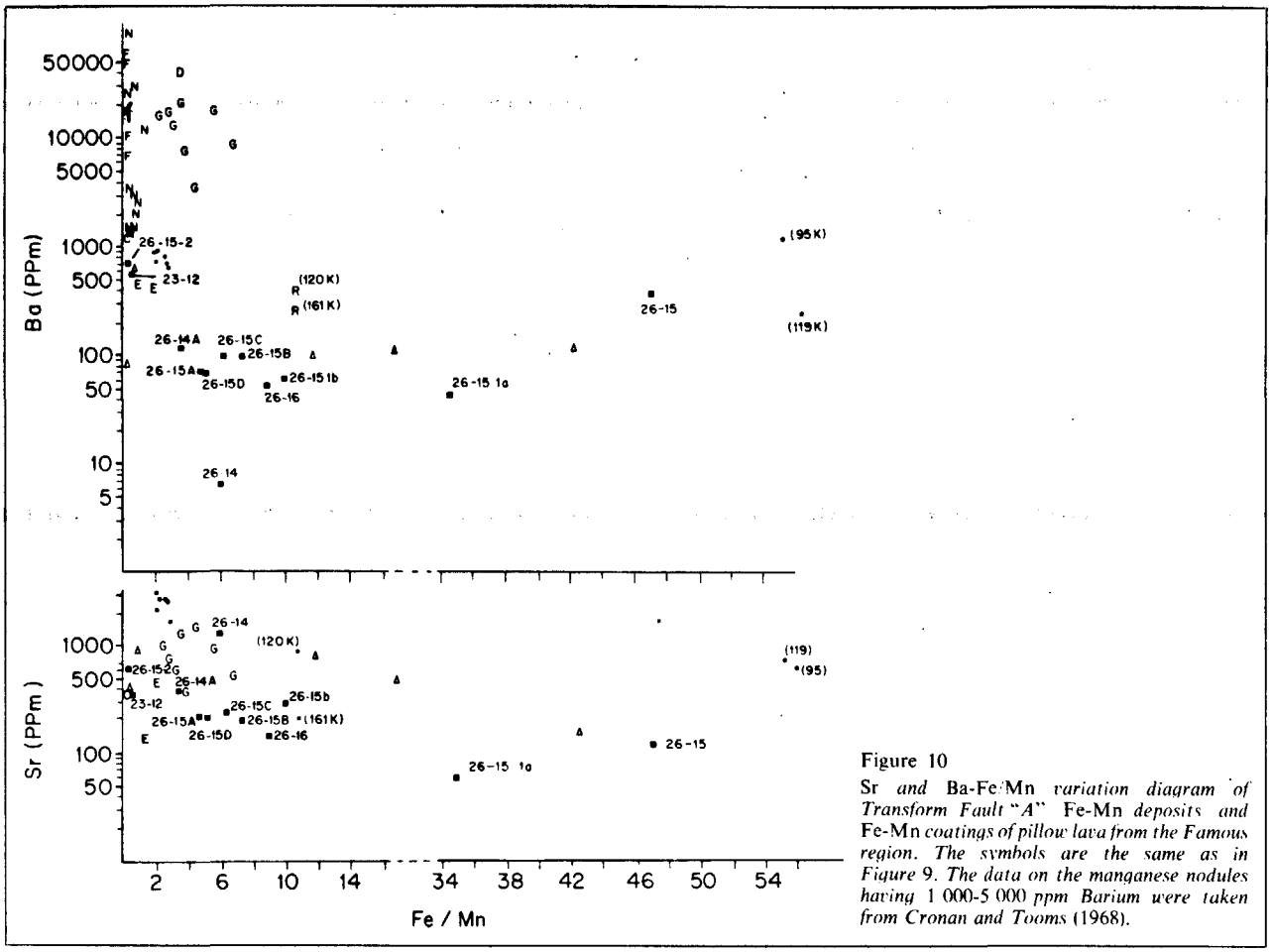

Figure 10

Sr and Ba-Fe/Mn variation diagram of Transform Fault "A" Fe-Mn deposits and Fe-Mn coatings of pillow lava from the Famous region. The symbols are the same as in Figure 9. The data on the manganese nodules having 1 000-5 000 ppm Barium were taken from Cronan and Tooms (1968).

Zinc

Zinc abundances show considerable variability among the different types of metalliferous deposits encountered in oceanic environments. Figure 9 suggests that there is a continuous decrease of Zn content from the nodules (1 500-3 000 ppm), to the Fe-Mn coatings of the basaltic rocks (279-424 ppm) and the hydrothermal deposits of Transform Fault "A" (6-126 ppm; Fig. 9; Table 2). Zinc is probably transported in solution and precipitates, together with Sr, Ba and Mn, in marine Fe-Mn hydrogenous deposits (e. g. nodules and Fe-Mn coatings on rocks). Co-precipitation of Mn, and Zn is also suggested by the relatively high concentration of zinc (Zn = 40-125 ppm) in the deposits of Transform Fault "A" characterized by Fe-Mn concretions (12, 15-2; Table 2, Fig. 9).

Cu, Ni and Co

The distribution of the transitional metals Cu, Ni and Co in the hydrothermal deposits from Transform Fault "A", the Fe-Mn coatings of pillows from nearby areas and other metalliferous deposits is shown by a ternary Fe-Mn (Cu + Ni + Co) diagram (Fig. 11). Most the hydrothermal samples from Transform Fault "A" fall in the Fe corner of the diagram, together with hydrothermal

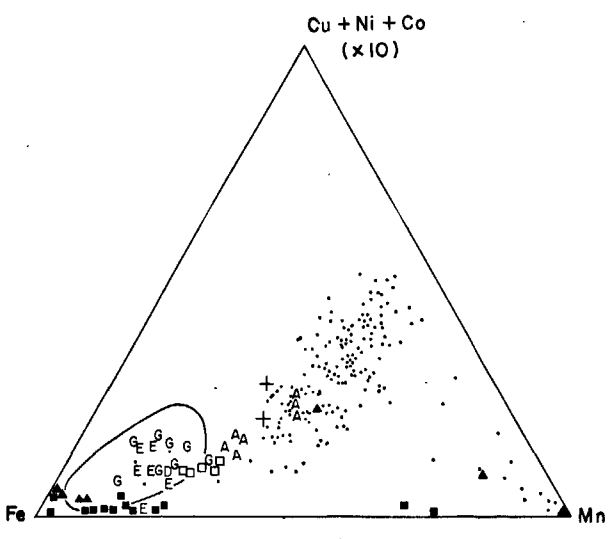

Figure 11

Ternary Fe-Mn (Cu + Ni + Co) diagram after Bonatti et al. (1972 b) showing the plots of Transform Fault "A" hydrothermal deposits (■) and of Fe-Mn coatings of basaltic rocks from the Famous area (□). E indicates data from the East Pacific Rise (Bostrom, Peterson, 1966). (+) indicates the Fe-Mn crusts from the Atlantis F. Z. (Scott et al., 1974). The black area in the Mn corner is the locus of points from the Mn-rich deposit of the TAG area near 26°N in the MAR (Scott et al., 1974) and those from the Afar region (Bonatti et al., 1972 a). The metalliferous deposits from the Red Sea fall within the encircled zone. Other symbols are as in Fig. 9.

deposits found at shallow ocean depths and on land (Banu Wuhu Volcano, Zelenov, 1965; Thera Caldera, Butuzova, 1966; Bonatti, 1972 *c*) and with the Fe-rich beds of the En-Kalafa region in Ethiopia (Bonatti *et al.*, 1972). It is interesting to note that the Fe-Mn coatings of basaltic rocks from the Famous area and some manganese crusts from the TAG area in the Atlantis fracture zone (Scott *et al.*, 1972) have overlapping values of Cu + Ni + Co (2 860-4 103 ppm and 4 140-5 635 ppm respectively), while others from the Atlantis fracture zone (TAG area) (Scott *et al.*, 1972) fall into the compositional field of the Pacific Ocean polymetallic nodules (Cu + Ni + Co = 8 629-19 520 ppm). Figure 11 shows that the broad field of polymetallic nodule composition has the shape of an inverted "V" (Fig. 11). However, the nodules are concentrated in a field of relatively high Cu + Ni + Co (Fig. 11). Intermediate values of Cu + Ni + Co (630-3 000 ppm) and Mn (0.5-6%) are encountered in the ferromanganoan deposits of the Bauer Deep (Sayles and Bischoff, 1973; Dymond *et al.*, 1973) and those of the Red Sea brines (Bischoff, 1969; Fig. 11). It is likely that the origin of the Red Sea brines is complex. Details on the complexity of this type of deposit are documented by Bischoff (1969) and by Bischoff and Manheim (1969). Chemically the Fe-Mn concretion type of material from Transform Fault "A" is closer to the manganese crust and the ferromanganese oxide found in the TAG area (Atlantis F. Z., Scott *et al.*, 1972) and those sampled from the Gulf of Aden (Cann *et al.*, 1977). The clay-rich hydrothermal deposits of Transform Fault "A" are similar to the mixed smectite-Mn-Fe oxide association found in the Gulf of Aden (Cann *et al.*, 1977). The presence of various types of hydrothermal material found together within the same samples, and often at the same location, suggests that a single source could give rise to separate material showing a large difference in Fe/Mn and Si/Al. These ratios are controlled by the overall chemical environments and the conditions of deposition, such as the pH of sea water, the temperature of discharge and the amount of iron in the source material. A common characteristic for the Transform Fault "A" hydrothermal deposits is their relatively low content of Cu, Ni and Co with respect to other known ocean floor polymetallic nodules and metalliferous sediment (Pacific Ocean nodules, Bauer Deep, Red Sea and the TAG area hydrothermal deposits).

CONCLUSION

1) Two hydrothermal deposits were found on the southern wall of Transform Fault "A", near the axial part of the transform valley and at a depth of about 2 700 m. Each of the two deposits extends over an area of about 600 m^2. The deposits are about 200 m apart. Direct field observation has shown that they build asymmetrical, elongated ridges 40 m long, 15 m wide and less than 3 m thick and with E-W fissure-like vents. The deposits occur in actively faulted terrain, and their young age is clearly associated with the continuing tectonic activity of the transform fault.

2) Two major types of deposit occur in both hydrothermal fields:

– black Fe-Mn concretions made up essentially of various manganese oxides and hydroxide minerals with a small amount of clay;

– a clay-rich hydrothermal material made up essentially of smectite, hydromica and small amounts of Fe-Mn concretions.

Both types of material are often intermixed and it is not uncommon to find layering of the clay-rich hydrothermal material with the Fe-Mn concretion-type of deposit.

3) Chemically the Fe-Mn concretions are distinguished from the clay-rich hydrothermal material by their higher Mn, Ba, V, Ni, Co and Cu content and their lower Fe, Si and K content.

4) Chemical and mineralogical zonation of the hydrothermal deposits is shown by the abundance of the clay-rich Fe-Si material near the vent and the increase in Fe-Mn concretion-type of material away from it. Among the Fe-Mn concretions, it is observed that the samples nearer to the vent consist of manganite, while away from the vent rancieite is more prominent.

5) Chemical analyses of Fe-Mn coatings of basaltic pillow lavas from the same general area show major compositional differences compared with the hydrothermal deposits. The Fe-Mn coatings of basaltic pillow lavas have lower Fe/Mn (2-3) and Si/Al (1.5-1.9) ratios than the clay-rich hydrothermal material. The transitional metal content is higher in the Fe-Mn coatings of rocks than in the hydrothermal deposits.

6) Comparative studies of different metalliferous deposits of the ocean floor should be considered with caution. At least three main types of deposits exist:

– hydrothermal deposits *sensu stricto* such as those from Transform Fault "A", the TAG area near 26°N (MAR), and the Fe-rich deposits of the EPR near 10°S, the Galapagos spreading center area and the Gulf of Aden;

– metalliferous sediments such as those from the Bauer Deep and the Red Sea;

– hydrogenous deposits such as the polymetallic nodules and the Fe-Mn coatings on basaltic rocks.

The hydrothermal deposits from Transform Fault "A" are, together with some of the metalliferous sediment of the Bauer Deep (Dymond *et al.*, 1973), the most Fe-rich deposits (Fe = 12-27%) encountered on the ocean floor with the exception of some of the Red Sea brines. It is also interesting to note that the hydrothermal deposits from Transform Fault "A" and the Mn-rich crusts from the TAG area near 26°N in the Atlantic Ocean (Scott *et al.*, 1974) are the most depleted in transitional metals such as Ni (570 ppm) when compared to known ocean floor metalliferous deposits, including polymetallic nodules and Bauer Deep and Red Sea deposits. The possible implications of this type of hydrothermal activity on the chemical budget of sea water are important and, although they have not been elaborated upon in this paper, they would be an interesting orientation for further work.

Acknowledgements

The hydrothermal deposits were found in Transform Fault "A" during the French-American Mid-Ocean Undersea Study (Famous), the French contribution to which was financed by the Centre National pour l'Exploitation des Océans (Cnexo). Special acknowledgement is made to the pilots of the diving saucer « Cyana » (R. Kientzy, G. Sciarrone) and to the diving engineers. The contributions of the captain, the officers and crew of R. V. « Le Noroit » (Cnexo) are likewise gratefully acknowledged. We thank C. Riffaud (Director for Cnexo of the Famous project) and Y. La Prairie (Président of Cnexo) for supporting the program. We are grateful to Y. Besnus, J. Samuel, R. Rouault, P. Staub, D. Trauth and I. Balouka at the University of Strasbourg (France) who made major and trace element analyses of the samples and performed the electron microscope work. Acknowledgement is made to H. Holland for discussions at sea and to H. Bougault who made some preliminary analyses of the samples and pointed out their remarkable depletion in transition elements. We thank N. Guillo and J. Le Gall for editorial assistance. M. Hoffert supervised the analytical work and, with A. Perseil, provided the mineralogical identifications.

REFERENCES

Arcyana, 1975. Transform fault and Rift valley from bathyscaph and diving saucer. *Science*, **190**, 108-116.

Arcyana, 1977. Rocks collected by bathyscaph and diving saucer in the Famous area of the Mid-Atlantic Rift valley: petrological diversity and structural setting. *Deep-Sea Res.*, **24**, 565-589.

Besnus Y., Lucas J., 1970. Méthode de dosage de 18 éléments majeurs et traces dans les roches sédimentaires et les produits d'altération par spectrométrie à lecture directe. *Colloques Nationaux du Cnrs.* **923**, 93-106.

Besnus Y., Rouault R., 1973. Une méthode d'analyse des roches au spectromètre d'arc à lecture directe par un dispositif d'électrode rotative. *Analusis*, **2**, 111-116.

Bischoff J. L., 1969. Red Sea geothermal brine deposits: their mineralogy, chemistry and genesis, in *Hot brines and recent heavy metal deposits in the Red Sea*, edited by E. T. Degens, D. A. Ross, Springer Verlag, Berlin, Heidelberg, New York, p. 368-401.

Bischoff J. L., Manheim F. T., 1969. Economic potential of the Red Sea heavy metal deposit, in *Hot brines and recent heavy metal deposits in the Red Sea*, edited by E. T. Degens, D. A. Ross, Springer Verlag, Berlin, Heidelberg, New York, p. 535-541.

Bischoff J. L., 1972. A ferroan nontronite from the Red Sea geothermal system. *Clays and clay miner.*, **20**, 217-223.

Bonatti E., Joensuu O., 1966. Deep-sea iron deposits from the South Pacific. *Science*, **154**, 643-645.

Bonatti E., Fisher D. E., Joensuu O., Rydell H., Bayth M., 1972 *a*. Iron-manganese-barium deposit from the northern Afar rift (Ethiopia). *Eco. Geol.*, **67**, 717-730.

Bonatti E., Kraemer T., Rydell H. S., 1972 *b*. *Classification and genesis of submarine iron-manganese deposits. Ferro-manganese deposits on the Ocean floor*, Lamont-Doherty Geological Observatory of Columbia University, Palisades, NY, 149-166.

Bonatti E., Honnorez J., Joensuu O., Rydell H. S., 1972 *c*. Submarine iron deposits from the Mediterranean Sea, in *Symposium volume on sedimentation in the Mediterranean Sea*, edited by D. J. Stanley, Internat. Sedimentology Cong., 8th, Heidelberg, 1971, 701-710.

Bostrom K., Peterson M. N. A., 1966. Precipitates from hydrothermal exhalations on the east Pacific Rises. *Econ. Geol.*, **61**, 1258-1265.

Butuzova G. Y., 1966. Iron-ore sediments of the fumarole field of Santorin volcano, their composition and origin. *Doklady. Adak. Nauk. SSSR*, **168**, 215-217.

Cann J. R., Winter C. K., Pritchard R. G., 1977. A hydrothermal deposit from the floor of the Gulf of Aden. *Mineral. Mag.*, **41**, 193-199.

Choukroune P., Francheteau J., Le Pichon X., 1977. Structural observation in an Oceanic Transform Fault from manned submersibles: Transform Fault "A" in the Famous area. *Geol. Soc. of Am. Bull.* (in press).

Cronan D. S., Tooms J. S., 1969. The geochemistry of manganese nodules and associated pelagic deposits from the Pacific and Indian Oceans. *Deep-Sea Res.*, **16**, 335-359.

Cronan D. S., 1975 *a*. Manganese nodules and other ferromanganese oxide deposits from the Atlantic Ocean. *J. Geophys. Res.*, **80**, 27?3831-3837.

Cronan D. S., 1975 *b*. Geological and geochemical factors determining the variability of marine manganese nodules. *3rd Oceanol. Internat.*, Brighton, 118-120.

Dymond J., Corliss J. B., Heath G. R., Field C. W., Dash E. J., Veeh H. H., 1973. Origin of metalliferous sediments from the Pacific Ocean. *Geol. Soc. of Am. Bull.*, **84**, 3355-3372.

Fein C. D., Morgenstein M., 1973. Microprobe analyses of manganese crust from the Hawaiian archipelago, in *Phase 1 report of inter-University program of research on ferromanganese deposits of the ocean floor*, 85-92.

Hajash A., 1975. Hydrothermal processes along mid-ocean ridges: an experimental investigation. *Contrib. Mineral. Petrol.*, **53**, 205-226.

Heath R. G., Dymond J., 1977. Genesis and transformation of metalliferous sediments from the East Pacific Rise, Bauer Deep and Central Basin, Northwest Nazca Plate. *Geol. Soc. Am. Bull.*, **88**, 723-733.

Hekinian R., Hoffert M., 1975. Rate of palagonitization and manganese coating on basaltic rocks from the Rift valley in the Atlantic near 36°50'N. *Mar. Geol.*, **19**, 91-109.

Krauskopf K. B., 1957. Separation of manganese from iron in sedimentary processes. *Geochim. Cosmochim. Acta*, **12**, 61-84.

Lalou C., Brichet E., Ku T. H., Jehanno C., 1977. Radiochemical scanning electron microscope (Sem) and X-ray dispersive energy (Edax) studies of Famous hydrothermal deposit. *Mar. Geol.* (in press).

Levinson A. A., Ludwick J. C., 1966. Speculation on the incorporation of B into argillaceous sediments. *Geochim. Cosmochim. Acta*, **30**, 855.

Michard G., 1975. L'action de l'eau de mer sur les basaltes, source possible de manganèse. Étude thermodynamique préliminaire. *CR Acad. Sc. Paris*, **280**, 1213-1216.

Moore J. G., 1966. Rate of palagonitization of submarine basalt adjacent to Hawaii. *US Geol. Survey Res. Paper*, 550 D, 163-171.

Moore W. S., Vogt P. R., 1976. Hydrothermal manganese crusts from two sites near the Galapagos spreading axis. *Earth Planet. Sci. Lett.*, **29**, 349-356.

Renard V., Schrumpf B., Sibuet J. C., Carré D., 1975. *Bathymétrie détaillée d'une partie de la vallée du Rift et de la faille transformante près de* 36°50'N *dans l'océan Atlantique*, Cnexo, Paris.

Rona P. A., 1977. Plate tectonics, energy and mineral resources: basic research leading to payoff. *Trans. Am. Geophys. Union*, **58**, 8, 629-639.

Sayles F. L., Bischoff J. L., 1973. Ferromanganoan sediments in the Equatorial East Pacific Rise. *Earth Planet. Sci. Lett.*, **19**, 330-336.

Scott R. B., Rona P. A., Butler L. W., Nalwalk A. J., Scott M. R., 1972. Manganese crusts of the Atlantis Fracture Zone. *Nature Phys. Sci.*, **239**, 92, 77-79.

Scott M. R., Scott R. B., Rona P. A., Butler L. W., Nalwalk A. J., 1974. Rapidly accumulating manganese deposit from the median valley of the mid-Atlantic Ridge. *Geophys. Res. Lett.*, **1**, 355-358.

Tanticelli L. A., Perkins R. W., 1973. Major and minor elemental composition of manganese nodules, in *Report 1 of Inter-University program research on ferromanganese deposits of the ocean floor*, 1-5.

Thompson G., Melson W. G., 1970. Boron contents of serpentinites and metabasalts in the oceanic crust: implications for the Boron cycle in the oceans. *Earth. Plan. Sci. Lett.*, **8**, 61-65.

Thompson G., Woo C. C., Sung W. Y., 1975. Metalliferous deposits on the Mid-Atlantic Ridge. *Geol. Soc. Am. Abstract*, 1297.

Zelenov K. K., 1965. Iron and manganese in exhalations of the submarine Banu Wuhu Volcano (Indonesia). *Doklady. Akad. Nauk. SSSR*, **155**, 94-96.